SEP
SECRETARÍA DE EDUCACIÓN PÚBLICA
Instituto Politécnico Nacional
"La Técnica al Servicio de la Patria"
ISSN: 1870-4069

RCS
Research in Computing Science

Vol. 67

Advances in Computing Science

E. A. Santos Camacho,
J. C. Chimal Eguía,
L. Cabrera Rivera,
E. Castillo Montiel, (Eds.)

Table of Contents

Índice

Databases & software Technology

Robotics and Mechatronics

Simulation & Modeling

Modeling Chemical Reactions and Heat and Mass Transport in a Hydrating Cement Particle Using Comsol Multiphysics 3.5a

Emilio Hernández–Bautista, Sadoth Sandoval–Torres, Prisciliano Felipe de Jesús Cano–Barrita.
Instituto Politécnico Nacional, CIIDIR Oaxaca
Hornos No. 1003, Col. Noche Buena, Santa Cruz Xoxocotlan, Oaxaca, México
Bautistahe@gmail.com

Abstract. A model based on the continuum mechanics theory was developed to describe the hydration reactions occurring in a cement particle surrounded by water. The heat and mass transfer in the particle was described by a diffusion–based mechanism. To solve the model, we considered the chemical reaction stoichiometry, which was then written using a chemical reaction engineering approach. The hydration reactions of C_3S and C_3A are exothermic, therefore they significantly contribute to the amount of energy in the domain. The equation system was solved by coupling the Reaction Engineering Lab Module to Comsol Multiphysics 3.5a. The results correctly describe the products formation and reactants consumption, simulating the formation of a shell around the unreacted cement particle, as well as the temperature evolution in the material. Also the model is capable of simulating the temperature increase in the whole system caused by the exothermic reactions.

Keywords. PID control, Fuzzy control, 2DOF PID control

1 Introduction

The process of curing concrete is meant to provide a high relative humidity and a suitable temperature in order to promote the cement hydration reactions. Steam curing at atmospheric pressure is routinely used in precast concrete plants, because it accelerates the cement hydration compared to curing at ambient temperature.

The concrete curing process has a significant influence in the properties of hardened concrete [1]. Adequate curing increases its durability, water–tightness, volume stability, mechanical strength, abrasion, and freezing and thawing resistance. However, during the steam curing process undesirable effects also occur during the hydration of cement. These are mainly moisture and temperature gradients that may cause micro-cracking, reducing the durability of the concrete elements.

The development of mathematical models of heat and mass transport during cement hydration is an essential tool for the study, design and optimization of new equipment, improving energy efficiency in transformation processes and reducing concrete deterioration by making it more impervious to aggressive agents.

For instance, various models have been developed to study the hydration of cement at a microscopic scale, such as the models developed by Bentz [2] and Van Breugel [3]. These models are capable of simulating the hydration of Portland cement

Advances in Computer Science and Engineering
Research in Computing Science 67, 2013 pp. 133–145
Paper Recived 16-08-2013 and Acepted 21-10-2013

particles. Other models incorporating heat and mass transport have been developed by [4] and [5].

The aim of this work is to develop a mathematical model that describes the transport mechanisms of moisture, heat transport and chemical reaction during curing of concrete with water vapor at atmospheric pressure. The focus of the model is a continuous type model to explain the transport phenomena occurring in the material thickness. The prediction of those variables will help us understand various phenomena occurring during hydration at the particle level, and then transferred to the material level. Moreover, the model proposed in this work will help understand the phenomena involving the differences in temperature and humidity profiles in concrete and propose steam curing procedures that minimize temperature and humidity gradients to prevent micro-cracking.

The first part of this paper presents the chemical engineering reaction for the hydration of cement without any spatial variation, the second part describes how the reactions are coupled to a 2-D model, showing its geometry, mass and energy balances, the constitutive equations, initial and boundary conditions, and the solution implementation by finite element in Comsol Multiphysics. The third part presents the simulation results for the species' concentration, the heat generated by hydration reactions and temperature evolution.

2 Development of the mechanistic model

The continuous medium is a physical description of the matter in which the domain can be described by a set of differential equations. The scale of the material can be represented from a set of molecules to volume scale of meters depending on the desired precision. Since the material is never continuous, the continuous medium approach is always an approximation to the actual phenomena.

A continuous type model is composed of a geometry, general balance equations of mass, energy or momentum, equations of state, boundary conditions and initial conditions of the system, and a set of assumptions that are necessary for the model development [6].

2.1 Chemical reaction engineering

The unreacted-core model for spherical particles of constant size was developed by Yagi and Kunii Paor [7], which consists of five phases. In cement hydration reactions only three of them occur: 1) Diffusion of water on the solid particles forming a thin film around the particle; 2) Diffusion and penetration of water through the reaction products on the surface of the particle; 3) reaction of water with the solid. The other two stages occur when the reaction products are in gaseous phase, but in this case we only have solid products. The reaction rate can be determined by any of these stages, so it is important to identify which of these control the process.

Stoichiometry of the chemical reaction in the hydration of cement: The cement phases generating hydration products upon contact with water that give early and subsequent compressive strength, and also generate most of the heat of reaction are:

3CaO SiO_2 (C_3S), 2CaO SiO_2 (C_2S) and 3CaO · Al_2O_3 (C_3A). Furthermore, these reagents comprise more than 80% of non-hydrated cement, and react according to the following stoichiometric equations:

$$2(3CaO{\cdot}SiO_2)+7H_2O=3CaO{\cdot}SiO_2{\cdot}3H_2O+3Ca(OH)_2 \quad \textbf{(1)}$$
$$2(2CaO{\cdot}SiO_2)+5H_2O=3CaO{\cdot}SiO_2{\cdot}3H_2O+Ca(OH)_2 \quad \textbf{(2)}$$
$$3CaO{\cdot}Al_2O_3+6H_2O=3CaO{\cdot}Al_2O_3{\cdot}6H_2O \quad \textbf{(3)}$$

Equations 1, 2 and 3 are modeled in the COMSOL Reaction Engineering Lab module to describe the disappearance of reactants and the appearance of hydrated products. This depends on the reaction stoichiometry and is described by Equation 4.

$$\frac{d(c_i V_r)}{dt} = V_r R_i \quad \textbf{(4)}$$

where c_i is the molar concentration of species i (mol/m^3), V_r is the reactor volume (m^3), t is time, and R_i is the rate of reaction (mol/m^3s), and i = C_3S, C_2S, C_3A, H, CSH, and C_3AH_6 COH. The above equation is a mass balance for each one of the species participating in the chemical reaction.

Note that this module does not model particle reaction, instead data related to reaction engineering and kinetics such as reaction time and heat generated as a function of time are obtained by considering that reactions are held in a 1m^3 batch reactor, perfectly mixed at 300 K.

Reactants: Equation 4 gives the material balance for the reactants in the mixed reactor. In this case the balance has a negative sign because of the decrease in concentration of these reactants during the course of the reaction (Equations 5-8).

$$\frac{d(c_{C3S})}{dt} = -2r_1 \quad \textbf{(5)}$$

$$\frac{d(c_{C3A})}{dt} = -r_3 \quad \textbf{(6)}$$

$$\frac{d(c_{C2S})}{dt} = -2r_2 \quad \textbf{(7)}$$

$$\frac{d(c_H)}{dt} = -7r_1 - 5r_2 - 6r_3 \quad \textbf{(8)}$$

Products: The balance of products has a positive sign because of its formation within the stirred reactor during the hydration (Equations 9-11).

$$\frac{d(c_{CSH})}{dt} = r_1 + r_2 \quad \textbf{(9)}$$

$$\frac{d(c_{COH})}{dt} = 3r_1 + r_2 \quad \textbf{(10)}$$

$$\frac{d(c_{C3AH6})}{dt} = r_3 \quad \textbf{(11)}$$

The reaction time depends on the reaction constant, which in turn depends primarily on the process conditions. In this case, the reaction conditions depend on the temperature, which is taken into account by the Arrhenius equation and is calculated with the rate constant k (Equation 12).

$$k = AT^n \exp(\frac{E}{R_g T}) \quad \textbf{(12)}$$

where A denotes the frequency factor, n is the temperature exponent, E is the activation energy (J / mol) and R_g is the ideal gas constant, 8.314J / (mol K). The value of the frequency factor for the reaction of tricalcium aluminate is $A = 1x10^{-5}$ [4], the exponent of the temperature is zero for $n = 0$ and the activation energy for the three reactions are: E = 100 J/mol, 155 J/mol, and 88 J/mol, for C_32, C_2S, and C_3A, respectively.

Once the rate constant is expressed as a function of temperature, the reaction rate is obtained as a function of the constant of reaction and concentration of the reactants. Equations 13-15 show that the reaction of C_3S is ninth order, c_C_3S is the concentration of tricalcium silicate and c_H_2O is the concentration of water. The concentration units are specified in moles. C_2S and C_3A reactions are seventh order.

$$r_1 = \mathrm{kf\_1*c\_C_3S^2*c\_H^7} \quad \textbf{(13)}$$

$$r_2 = \mathrm{kf\_2*c\_C_2S^2*c\_H^5} \quad \textbf{(14)}$$

$$r_3 = \mathrm{kf\_3*c\_C_3A*c\_H^6} \quad \textbf{(15)}$$

In order to get the heat of reaction, it is necessary to establish the thermochemical of the reaction, by calculating the reaction enthalpy from each of the reactions, obtained by subtracting the enthalpy of the less reactive products. Equation 16-18.

$$H_{reaccionC3S} = \mathrm{-2h\_C3S + h\_CSH + 3h\_COH - 7h\_H} \quad \textbf{(16)}$$

$$H_{reaccionC2S} = \mathrm{h\_CSH + h\_COH - 2h\_C2S - 5h\_H} \quad \textbf{(17)}$$

$$H_{reaccionC3A} = \mathrm{-h\_C3A - 6h\_H + h\_C3AH6} \quad \textbf{(18)}$$

The maximum heat generated during these reactions is thus calculated. If negative, we refer to an exothermic reaction [7], which releases heat to the outside.
Then the heat generated is calculated and will depend on the reaction rate r of each chemical reaction and the concentration of each of the reactants. Heat generated by chemical reactions is expressed by equation 19.

$$Q = -V_r \sum_j H_j r_j \quad \textbf{(19)}$$

Substituting equations 16 to 18 in equation 19 would provide the heat generated by the reaction.

$$Q = -V_r \left(H_{reaccionC3S} r_1 + H_{reaccionC2S} r_2 + H_{reaccionC3A} r_3 \right) \quad \textbf{(20)}$$

2.2 Model geometry

Model geometry is shown in Figure 1. It consists of one cement particle having a 0.005 m diameter and surrounded by water in a closed system represented by a square of 0.01 m. Therefore, the domain Ω of the system is composed of two subdomains (subdomain Ω1 for water and subdomain Ω2 for cement) and 4 external boundaries δΩ, 3 internal borders δΩ and 10 points $\delta^2\Omega$.

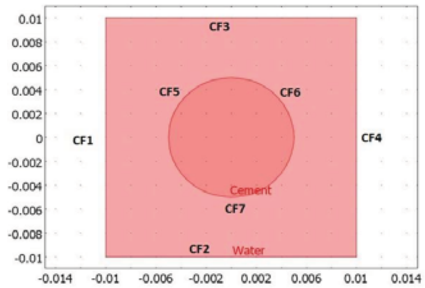

Fig. 1. Cement particle geometry.

The hydration chemical reactions of C_3S, C_2S and C_3A occur only in the domain of the particle.

2.3 Mass and energy balances

Mass transfer in the geometry shown in Figure 1 occurs primarily by diffusion of the species participating in the chemical reaction. The equation describing the transport of all species in the model is as follows (Equation 21):

$$\delta_{ts}\frac{\partial c_i}{\partial t}+\nabla\left(-D_i\nabla c_i\right)=R_j \tag{21}$$

where c is the concentration of species i participating in the reaction either as a product or as a reactant, D_i is the diffusion coefficient for each species i, and j is the reaction rate j = 1, 2 and 3 for C_3S, C_2S and C_3A, respectively. The process can be anisotropic and in this case, $\boldsymbol{D}$ has to be considered as a tensor. However this model only considers the medium as isotropic because of the domain size. In our model we have seven equations that correspond to the number of chemical species in the system domain.

Regarding the heat equation (Eq. 22), it is considered that the energy is transported mainly by conduction in both the domain of the particle and the domain of water.

$$\delta\rho C_p\frac{\partial T}{\partial t}+\nabla\left(-k\nabla T\right)=Q \tag{22}$$

where δ is a temporal scaling coefficient (dimensionless), ρ is the density of the cement paste and hardened cement kg/m^3, C_p is the specific heat capacity at constant pressure (J/kgK), k is the thermal conductivity (W/mK), and Q (W/m^3) contains the heat source due to the chemical reaction of C_3S, C_2S and C_3A, Eq. 20. The thermal conductivity may be anisotropic, however in this model it is considered to be isotropic in the direction of heat flow.

2.4 Equations of state

As a first approximation the diffusion coefficients in the cement paste were considered constant and are given in Table 1.

Table 1. Density and diffusion coefficient of the phases in the cement paste

Phase	Density (kg/m^3)	Diffusion coefficient (m/s^2)
C_3S	3150	$1X10^{-20}$
C_2S	3310	$1X10^{-20}$
C_3A	3030	$1X10^{-20}$
H	1000	$1X10^{-5}*(r_1+r_2+r_3)$
CSH	2350	$1X10^{-20}$
COH	2240	$1X10^{-20}$
C_3AH_6	2520	$1X10^{-20}$

Diffusion coefficient: The diffusion coefficients of the chemical species in the cement are from $1.0E^{-20}$ to $1.0E^{-5}$ m^2/s [6]. The diffusion coefficient of water in the domain is described as a function of reaction rates as shown in Table 1. The reaction rate decreases during the hydration process because the products such as CSH, COH and C_3AH_6 cover the cement particle surface and prevents water from penetrating and reaching the unreacted cement.

Thermal conductivity and specific heat: The thermal conductivity of concrete is considered constant, with a value of 3 W / (m · K) and densities of water and cement are 1000 kg/m^3 and 3000 kg/m^3 respectively. The heat capacity of water and cement are 4200 J/kgK and 2000 J/kg K, respectively.

2.5 Boundary and initial conditions

The system begins with initial conditions of a concentration of 6 mol/m^3 H_2O and a concentration of 3 mol/m^3 C_3S at a temperature of 300 K. In Figure 1 we show the geometry of the model, consisting of two subdomains, the domain of water and the domain of cement where reactions, heat and mass transport occur. In the domain of water heating only occurs by the release of energy from the particle.

Table 2. Initial conditions for subdomains

Phase	Initial concentration mol/m^3 ($\delta\Omega 1$)	Initial concentration mol/m^3 ($\delta\Omega 2$)
C_3S	0	3
C_2S	0	2
C_3A	0	1
H	6	0
CSH	0	0
COH	0	0
C_3AH_6	0	0

The initial concentrations in the two subdomains of the model are shown in Table 2. It can be observed that the concentrations of the products are zero at the start of the reaction at time zero. The C_3S, C_2S, and C_3A contents for the cement used were calculated according to the Bogue equations [1].

The system has four internal and three external contours as shown in Figure 1. The boundary conditions of each of the diffusion equations for the species *i*, are expressed in equations 23 to 26 as follows:

External border conditions for species, i = C_3S, C_2S, C_3A, H_2O, CSH, COH and C_3AH_6 are insulated and no exchange of matter with the environment occurs. In Figure 1, these boundaries are marked as CF1, CF2, CF3 and CF4, and the conditions are expressed for each compound *i*, as follows.

$$\mathbf{n}\cdot\left(-D_i\nabla c_i\right)=0 \quad \text{Over } \delta\Omega1 \tag{23}$$

For internal boundary conditions CF5, CF6 and CF7, boundary conditions depend on the concentration of reactants and products in the subdomain Ω1 (water) and in the subdomain Ω2 (cement). Because the concentrations are an extension of the interaction of the two domains is said to be a continuous boundary condition.

$$\mathbf{n}\cdot\left[\left(-D_i\nabla c_i\right)_{\Omega1}-\left(-D_i\nabla c\right)_{\Omega2}\right]=0 \quad \text{Over } \delta\Omega2 \tag{24}$$

For the energy balance, boundary conditions are similar to the conditions used in the mass transport equations (23–24). The boundary conditions for exterior boundaries are thermal insulation and conditions for internal contours are continuous type boundary conditions, and they are given in equations 25 and 26.

$$\mathbf{n}\cdot\left(K\nabla T\right)=0 \quad \text{Over } \delta\Omega1 \tag{25}$$

$$\mathbf{n}\cdot\left[\left(K\nabla T\right)_{\Omega1}-\left(K\nabla T\right)_{\Omega2}\right]=0 \quad \text{Over } \delta\Omega2 \tag{26}$$

2.5 Solution

COMSOL Multiphysics 3.5a, which has methods based on finite element solution, was used to solve the partial differential equations system in the domain. The solution was obtained by the following steps [8, 9].

- Discretization of continuous media: The geometry was divided into 989 elements and set a time step of 1 s, and started from 0 to 1000s. The computation time was 54.84s
- Selecting an interpolation function: The preset interpolation function in Comsol Multiphysics 3.5a is a function for two-dimensional triangular quadratic polynomial represented by a LaGrange polynomial.

$$T=\alpha_1+\alpha_2x+\alpha_3y+\alpha_4x^2+\alpha_5y^2+\alpha_6xy \tag{27}$$

- Establishing the mathematical formulation of the partial differential equations in matrix form.
- Assembling the basic equations for a system of simultaneous equations.

- Solving the system of equations: Using UMFPACK code incorporated into COMSOL Multiphysics 3.5a, which is the code for sparse nonlinear systems.
- Calculating secondary quantities such as space heat fluxes, space concentration fluxes, etc.

3 Simulation results from the hydration of a cement particle

3.1 Chemical reactions

We obtained the main reaction kinetics in the module Reaction Engineering Lab, shown in Figure 2. This plot shows the evolution of the concentration of reactants in a batch reactor of 1 m^3 of volume.

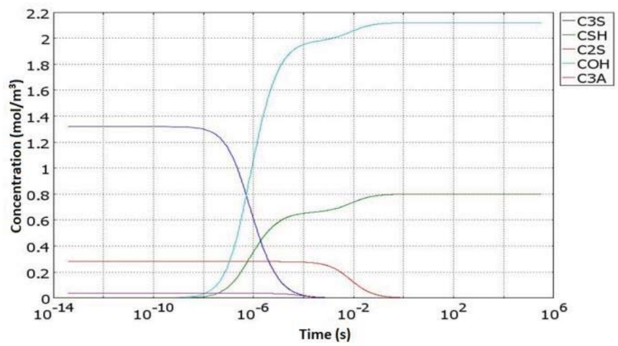

Fig. 2. Reaction kinetics of the species modeled in COMSOL Multiphysics 3.5a.

The graph shows the evolution of reactants C_3S, C_2S, C_3A and the products CSH, COH, and C_3AH_6. As can be observed the product formation does not contemplate the dormant period [10], because having the assumption of a continuous stirred reactor, products react within seconds when they reach the last part of kinetics. Generating calcium silicate hydrate and calcium hydroxide consists of two phases: first when it is generated due to the reaction of tricalcium silicate, and the second due to the reaction of dicalcium silicate. In water there are also different stages in the reaction kinetics (not shown in Figure 2.), which are the result of the C_3S, C_3A and C_2S reactions.

3.2 Evolution of reactants in the cement particle

We simulated the hydration reaction in a cement particle, from 0 s to 1000s, using the kinetic data obtained in the Reaction Engineering Lab Module, as mentioned above. Figure 3 shows that the concentration of reactants is high only in the core after 100 s (Figure 3 left) and is represented by red color. The concentration decreases with respect to time. In a time of 1000s the C_3S concentration in the core starts to decrease.

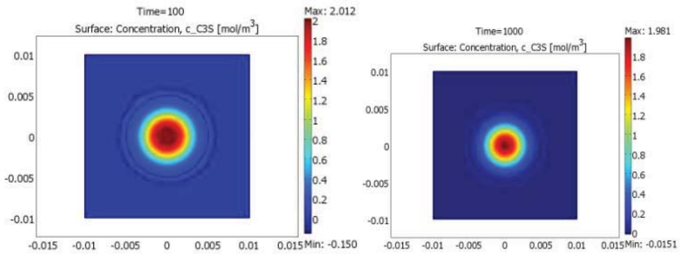

Fig. 3. Spatial evolution of the concentration of C_3S of during hydration of a particle (left 100s, 1000s right).

In the case of the reaction of C_2S, Figure 4, the reaction occurs slower due to the low activation energy involved in the chemical reaction.

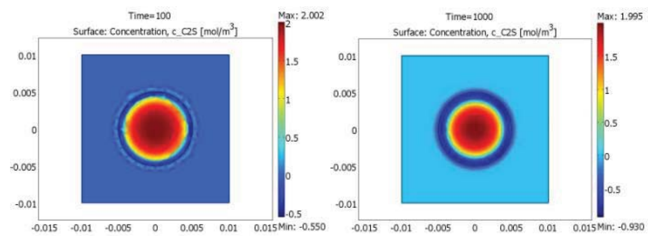

Fig. 4. Spatial evolution of the concentration of C_2S of during hydration of a particle (left 100s, 1000s right).

The C_3A is at lower concentration in the reactions, but the reaction rate in the particle is faster than the C_2S and C_3S reactions (Figure 5).

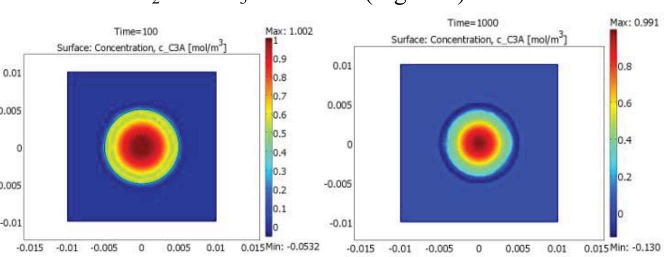

Fig. 5. Spatial evolution of the concentration of C_3A of during hydration of a particle (left 100s, 1000s right)

3.3 Evolution of products in the cement particle

Regarding the evolution of products, it can be observed that the calcium silicate hydrate increases the particle surface rapidly since it is occurring in two reactions of Equation 1 and Equation 2. Thus, molar concentration of CSH increases by the contribution of C_3S and C_2S reactions Figure 6.

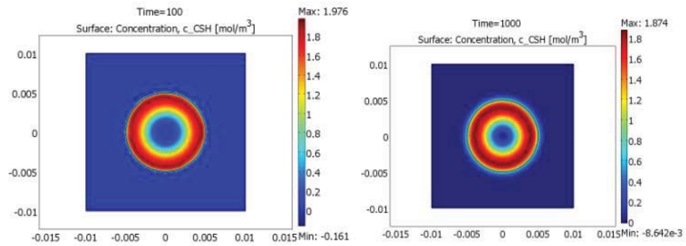

Fig. 6. Spatial evolution of the concentration of CSH of during hydration of a particle (left 100s, 1000s right).

The concentration of calcium hydroxide (COH) will increase twice compared to the concentration of calcium silicate hydrate Figure 7. However, this increase is only in concentration because the amount of calcium silicate hydrate is in higher proportion, since the molecular weight is much larger than C_3S.

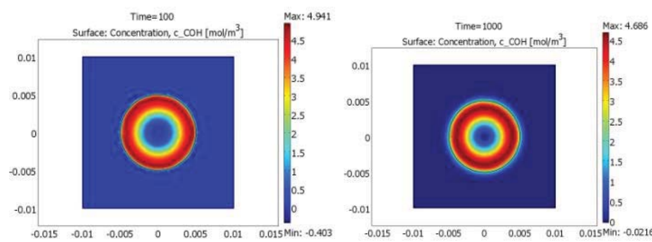

Fig. 7. Spatial evolution of the concentration of COH of during hydration of a particle (left 100s, 1000s right)

The concentration of tricalcium aluminate hydrated products C_3AH_6, Figure 8, will have a slow increase in the border of the particles, due to the low reactant concentration, and at 1000s just begins to react around the core.

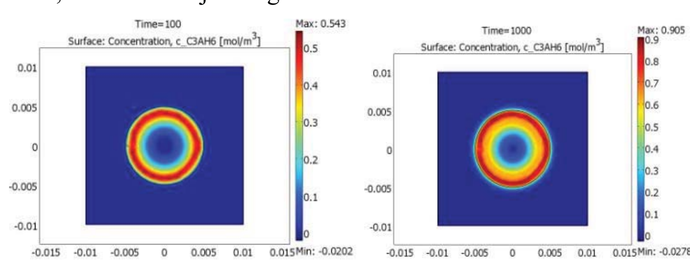

Fig. 8. Spatial evolution of the concentration of C_3AH_6 of during hydration of a particle (left 100s, 1000s right).

3.4 Temperature

Due to heat generation by the exothermic reactions at the surface of the particle, the water domain starts a heating period at approximately 100s. Figure 9 shows the direction of heat flux (red lines). It is important to see that the heat flux is increased in the surface, as shown by larger arrows in the surface. These arrows are moved to the center, which indicates that heat flow after 1000s is mainly inside the particle.

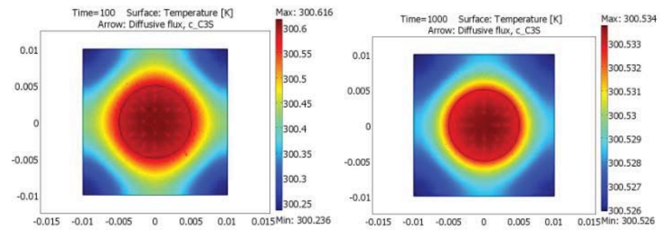

Fig. 9. Spatial evolution of the temperature and heat flow during hydration of a particle (left 100s, 1000s right)

Figure 10 shows the increase in temperature at different points of the radius of the particle, $1.25x10^{-3}$ $2.5\ x10^{-3}$ $3.7\ x10^{-3}$, at the surface 0.005m and at the water domain. It is observed that the temperature changes rapidly from 300 K to 301.2 K, due to heat generation on the surface. This flow of heat generated is conducted to the water, because of the continuity conditions shown in Equation 26. Since concrete is a self–heating material, the heat generation rate is much larger than the rate of heat loss at the boundaries. This happens due to the particular thermal conductivity and specific heat capacity, therefore heat generation occurs at the surface, where there is a loss of heat in the medium. The surface reaches 301.2 K ($5x10^{-3}$m), and as we approach the core, the temperature begins to decrease because the nucleus reactions have not been carried out or not completed ($1.25x10^{-3}$m).

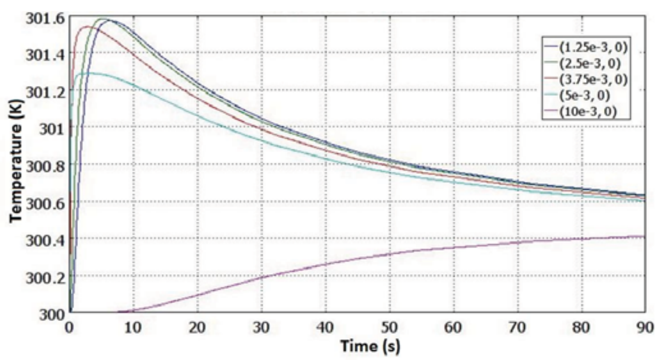

Fig. 10. Evolution of temperature during the time in four points on the radius of the particle.

Now if we compare the external boundary of the domain of water ($10x10^{-3}$), we see that there is a temperature increase. We should clarify that the heat transfer at the cement particle-water interface, and at the water domain the heat transfer occurs by conduction, so it is considered that there is no water movement (buoyancy effect)[11].

4 Conclusion

A model for hydration of a cement particle, transport of matter and energy has been developed based on an approximation of the continuous type. This model describes the hydration of a particle with a radius of 0.01m, which is surrounded by water.
The model describes the chemical reactions, evolution of heat, diffusion of chemical species in a circular geometry. The model involves the reaction of C_3S, C_2S, and C_3A.When considering these reactions a higher rate is shown, resulting in a rapid generation of heat, which propagates into the medium. The incorporation of the three species mainly contributes to the generation of CSH and COH, as C_3S and C_2S contributes to an increase in the generation of this products. In addition, the incorporation of the C_3A leads to increased heat generation.

Acknowledgments

Emilio Hernández Bautista acknowledges Conacyt for the PhD scholarship and to the Instituto Politecnico Nacional for the PIFI scholarship.

References

1. Mehta, P. K. , and Monteiro, P. J. M: Concrete Microestructure, properties, and Materials, Third Edit. New York USA (2006) p. 644.
2. Bentz, D. P.: CEMHYD3D: A Three-Dimensional Cement Hydration and Microstructure Development Modeling Package . Version 3 . 0, Nist (2005) p. 234.
3. Chen, W.: Hydration of slag cement Theory, Modeling and Application, (2006) p. 223.
4. Zhang, B. , and Yu, X. : Multiphysics for Early Stage Cement Hydration: Theoretical Framework. Advanced Materials Research (2011) p 4247.
5. Maekawa, K., and Ishida,: Multi-scale Modeling of Concrete Performance Integrated Material and Structural Mechanics. Journal of Advanced Concrete Technology (2003) p 670.
6. Bear, J., Cheng, H. D.: Modeling Groundwater Flow and Contaminant Transport. Springer (2010) p 834.
7. Levenspiel, O.: Ingenieria de las Reacciones Quìmicas. Limusa Wiley, third edition (2002) p. 638.
8. Baker, A. J. : Finite Elements Computational Engineering Sciences. Wiley, first edition (2012) p 873.
9. Battaglia, J.-L.: Heat Transfer in Materials Forming Processes. University of Bordeaux, France (2008), p. 358.
10. Smilauer, V., Krejci, T.: Multiscale model for temperature distribution in hydrating concrete. International Journal for Multiscale Computational Engineering (2009) p 135.
11. Tritt, T. M.: Thermal conductivity, First edition. United States (2005) p. 153.